Ultrabroadband pulse shaping with a push-pull deformable mirror

Stefano Bonora,[1,*] Daniele Brida,[2] Paolo Villoresi,[1] Giulio Cerullo[2]

[1]*IFN-CNR, Laboratory for Ultraviolet and X-Ray Optical Research, D.E.I. – Università degli studi di Padova, Padova, Italy*

[2]*IFN-CNR, Dipartimento di Fisica, Politecnico di Milano, Piazza Leonardo da Vinci 32, 20133 Milano, Italy*

**bonox@dei.unipd.it*

Abstract: We report the programmable pulse shaping of ultrabroadband pulses by the use of a novel design of electrostatic deformable mirror based on push pull technology. We shape few-optical pulses from near-IR and visible optical parametric amplifiers, and demonstrate strong-field control of excited state population transfer in a dye molecule.

OCIS codes: (320.5540) Pulse shaping; (320.7160) Ultrafast technology; (010.1080) Adaptive optics.

References and links

1. A. M. Weiner, "Femtosecond pulse shaping using spatial light modulators," Rev. Sci. Instrum. **71**(5), 1929–1960 (2000).
2. Y. Silberberg, "Quantum coherent control for nonlinear spectroscopy and microscopy," Annu. Rev. Phys. Chem. **60**(1), 277–292 (2009).
3. A. Assion, T. Baumert, M. Bergt, T. Brixner, B. Kiefer, V. Seyfried V, M. Strehle, and G. Gerber, "Control of chemical reactions by feedback-optimized phase-shaped femtosecond laser pulses," Science **282**(5390), 919–922 (1998).
4. J. A. Salehi, A. M. Weiner, and J. P. Heritage, "Coherent ultrashort light pulse code-division multiple access communication systems," J. Lightwave Technol. **8**(3), 478–491 (1990).
5. A. M. Weiner, D. E. Leaird, J. S. Patel, and J. R. Wullert, "Programmable femtosecond pulse shaping by use of a multielement liquid-crystal phase modulator," Opt. Lett. **15**(6), 326–328 (1990).
6. C. W. Hillegas, J. X. Tull, D. Goswami, D. Strickland, and W. S. Warren, "Femtosecond laser pulse shaping by use of microsecond radio-frequency pulses," Opt. Lett. **19**(10), 737–739 (1994).
7. P. Tournois, "Acousto-optic programmable dispersive filter for adaptive compensation of group delay time dispersion in laser systems," Opt. Commun. **140**(4-6), 245–249 (1997).
8. E. Frumker, E. Tal, Y. Silberberg, and D. Majer, "Femtosecond pulse-shape modulation at nanosecond rates," Opt. Lett. **30**(20), 2796–2798 (2005).
9. B. J. Pearson, and T. C. Weinacht, "Shaped ultrafast laser pulses in the deep ultraviolet," Opt. Express **15**(7), 4385–4388 (2007).
10. S.-H. Shim, D. B. Strasfeld, and M. T. Zanni, "Generation and characterization of phase and amplitude shaped femtosecond mid-IR pulses," Opt. Express **14**(26), 13120–13130 (2006).
11. E. Zeek, K. Maginnis, S. Backus, U. Russek, M. Murnane, G. Mourou, H. Kapteyn, and G. Vdovin, "Pulse compression by use of deformable mirrors," Opt. Lett. **24**(7), 493–495 (1999).
12. J. Garduño-Mejía, A. H. Greenaway, and D. T. Reid, "Programmable spectral phase control of femtosecond pulses by use of adaptive optics and real-time pulse measurement," J. Opt. Soc. Am. B **21**, 833–843 (2004).
13. P. Wnuk, C. Radzewicz, and J. S. Krasiński, "Bimorph piezo deformable mirror for femtosecond pulse shaping," Opt. Express **13**(11), 4154–4159 (2005).
14. G. Cerullo, and S. De Silvestri, "Ultrafast optical parametric amplifiers," Rev. Sci. Instrum. **74**(1), 1–18 (2003).
15. A. Baltuška, T. Fuji, and T. Kobayashi, "Visible pulse compression to 4 fs by optical parametric amplification and programmable dispersion control," Opt. Lett. **27**(5), 306–308 (2002).
16. D. Brida, G. Cirmi, C. Manzoni, S. Bonora, P. Villoresi, S. De Silvestri, and G. Cerullo, "Sub-two-cycle light pulses at 1.6 microm from an optical parametric amplifier," Opt. Lett. **33**(7), 741–743 (2008).
17. D. Brida, S. Bonora, C. Manzoni, M. Marangoni, P. Villoresi, S. De Silvestri, and G. Cerullo, "Generation of 8.5-fs pulses at 1.3 microm for ultrabroadband pump-probe spectroscopy," Opt. Express **17**(15), 12510–12515 (2009).
18. S. Bonora, and L. Poletto, "Push-pull membrane mirrors for adaptive optics," Opt. Express **14**(25), 11935–11944 (2006).
19. S. Bonora, I. Capraro, L. Poletto, M. Romanin, C. Trestino, and P. Villoresi, "Wave front active control by a digital-signal-processor-driven deformable membrane mirror," Rev. Sci. Instrum. **77**(9), 093102 (2006).
20. C. Manzoni, D. Polli, and G. Cerullo, "Two-colour pump-probe system broadly tunable over the visible and the near infrared with sub-30-fs temporal resolution," Rev. Sci. Instrum. **77**(2), 023103 (2006).

#132628 - $15.00 USD Received 30 Jul 2010; revised 17 Sep 2010; accepted 20 Sep 2010; published 19 Oct 2010

21. D. J. Tannor, and S. A. Rice, "Control of Selectivity of Chemical Reaction via Control of Wave Packet Evolution," J. Chem. Phys. **83**(10), 5013–5018 (1985).
22. R. W. Gerchberg, and W. O. Saxton, "A practical algorithm for the determination of the phase from image and diffraction plane pictures," Optik (Stuttg.) **35**, 237–246 (1972).
23. S. Fechner, F. Dimler, T. Brixner, G. Gerber, and D. J. Tannor, "The von Neumann picture: a new representation for ultrashort laser pulses," Opt. Express **15**(23), 15387–15401 (2007).
24. G. Cerullo, C. J. Bardeen, Q. Wang, and C. V. Shank, "High power chirped pulse excitation of molecules in solution," Chem. Phys. Lett. **262**(3-4), 362–368 (1996).
25. C. J. Bardeen, Q. Wang, and C. V. Shank, "Femtosecond Chirped Pulse Excitation of Vibrational Wave Packets in LD690 and Bacteriorhodopsin," J. Phys. Chem. A **102**(17), 2759–2766 (1998).

1. Introduction

Femtosecond pulse shaping [1] is a key technology in ultrafast science, enabling many applications such as non linear spectroscopy and microscopy [2], coherent control of photochemical processes [3] and optical communications [4]. Several devices have been proposed for the synthesis of shaped pulses, such as Liquid Crystals Spatial Light Modulators (LC-SLMs) [5] Acousto-Optic Modulators (AOMs) [6], Acousto-Optic Programmable Dispersive Filters (AOPDFs) [7] and electro-optical phase arrays [8]. LC-SLMs have a very high spectral resolution and provide both phase and amplitude modulation, thus allowing the generation of very complex pulse shapes. On the other hand, the pixelization of the device leads to diffraction losses and to the formation of pulse wings and pedestals; in addition, their transparency range is limited from 430 nm to 1600 nm, excluding the important IR and UV frequency ranges. AOMs and AOPDFs exploit modulation of a sound wave propagating in a crystal to manipulate both spectral phase and amplitude of the diffracted beam. Depending on the used crystal, they can operate in different spectral regions from the UV [9] to the mid-IR [10], and they provide a very high number of effective "pixels". However their throughput is rather low, since they rely on the diffracted light, each spectral range requires its dedicated device and the capability to handle broad bandwidths comes at the expense of diffraction efficiency, which can be as low as 10% for octave-spanning bandwidths.

Deformable mirrors (DMs) rely on the smooth phase variations induced by the deformation of a thin membrane [11,12] or of a semi-passive bimorph structure [13]. Both technologies present nearly the same performances with respect to number of electrodes and maximum deformations. Although DMs have limited spectral resolution and can be used just for phase modulation, they have the important advantages of supporting ultrabroad bandwidths with high throughput and of being substantially achromatic, with spectral coverage from the UV to the mid-IR limited only by the reflectivity of the metallic coating. Their flexibility of use makes them particularly suitable for sources of tunable ultra-broadband pulses such as Optical Parametric Amplifiers (OPAs) [14]. Conventional DMs have one row of electrostatic actuators facing the membrane, thus allowing only a limited stroke and relatively simple deformations; this makes them particularly suited to pulse compression to the transform-limited (TL) duration, for which simple polynomial (up to fourth/fifth order) spectral phase profiles are required [11,15–17]. However true pulse shaping has not been demonstrated so far with DMs because it requires control on the deformation up to high polynomial orders, thus calling for higher DM strokes combined with push-pull capabilities.

In this paper we employ a novel push-pull DM design, extending the scheme recently introduced by some of the authors [18], in which the actuators are pulling both sides of the membrane. This allows for deformations in both directions, unlike the single-side deformation possible with the standard electrostatic DMs, thus enabling the synthesis of much more complex spectral phase profiles. We here demonstrate the capability of the push-pull DM to shape ultrabroadband pulses generated by non-collinear OPAs (NOPAs) in the near-IR and visible spectral ranges. We also apply the DM-based pulse shaper to strong field coherent control of population transfer in a dye molecule.

#132628 - $15.00 USD Received 30 Jul 2010; revised 17 Sep 2010; accepted 20 Sep 2010; published 19 Oct 2010

2. Double side deformable mirror

The design of the push-pull DM is shown in Fig. 1. It consists of a 5-μm-thick silver-coated nitrocellulose membrane, faced on both sides by arrays of linear electrodes. The metallic coating of the membrane is electrically connected to the ground, forming a capacitor with both electrodes arrays. The front electrodes push the membrane to positive deformations (i.e. the membrane moves towards the incoming light beam) while the back electrodes pull the membrane to negative deformations.

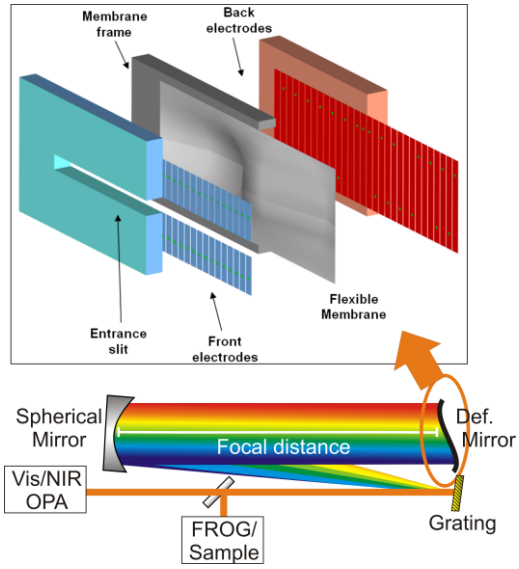

Fig. 1. Sketch of the experimental setup for pulse shaping with exploded view of the push-pull membrane deformable mirror. The actuators geometry is 15mm × 40mm. The slit size is 2mm × 40mm.

To avoid the transmission of the pulse through the transparent electrode as in Ref [18], here the laser light reaches the mirror through a slit (2mm × 40mm) in the center of the top electrode array. The electrodes on the bottom side are spaced by 140 μm from the membrane, while the spacing of the top-side electrodes is reduced to 100 μm to compensate for their smaller area, necessary to accommodate the slit. The DM has 30 actuators on the bottom side (1.2mm × 15mm, 0.3mm spaced) and 30 actuators on the top side facing the other ones. The actuators are driven by two arrays of 30 independently addressable high-voltage amplifiers providing up to 300 V each.

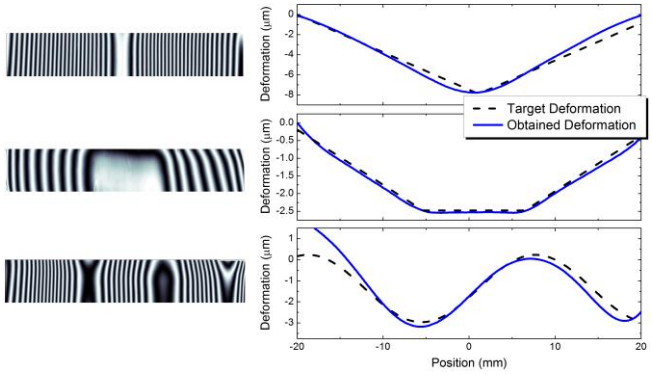

Fig. 2. Interferograms of the deformed mirror (45 × 2 mm) on the left, and comparison between the target (black dashed line) and the measured deformation (blue solid line) on the right. The target deformations are, from top, triangular, flat bottom and sine.

#132628 - $15.00 USD Received 30 Jul 2010; revised 17 Sep 2010; accepted 20 Sep 2010; published 19 Oct 2010

The DM has been initially characterized by a Twyman-Green interferometer [19]. The maximum stroke was found to be 9μm for the front electrodes and 8.5μm for the back ones. The deformation given by each actuator was measured and stored in the influence functions matrix which is then used for the determination of the mirror shape under linear approximation [17]. The degree of control in mirror deformation that we achieved with this approach is demonstrated in Fig. 2, which shows a comparison between target and measured mirror deformations for different mirror shapes, corresponding to triangular, flat bottom and sinusoidal phase profiles. An even better agreement could be achieved by an iterative approach. Note that, by exploiting the pulling action from both sides of the membrane, it is possible to realize much more complex patterns that would not be possible with a single-sided DM.

3. Experimental setup for ultrabroadband pulse shaping

To demonstrate the flexibility and broad acceptance bandwidth of our DM pulse shaper, we interfaced it to nearly single-cycle pulses generated by NOPAs in the near-IR and in the visible, both driven by an amplified Ti:sapphire laser (0.6 mJ, 150 fs pulses at 780 nm and 1 kHz). The near-IR NOPA has been described in detail elsewhere [17]. Briefly, a white light seed generated in a sapphire plate is amplified in a 1.2-mm-thick periodically poled stoichiometric lithium tantalate crystal pumped by the fundamental frequency of the laser. The non-collinear angle (1.9° internal) and the poling period (20.9 μm) are chosen to achieve a broad gain bandwidth in the near-IR through group-velocity matching of signal and idler pulses [14] at 1.3 μm wavelength. The NOPA generates 2-μJ ultra-broadband pulses with spectrum extending from 1.1 to 1.7 μm (see Fig. 3(b)). For the experiments reported in Section 5 we used a standard second-harmonic pumped visible NOPA with a chirped mirror compressor, described in detail in Ref [20]. The pulse shaper consists in a 4*f* configuration with a 150 lines/mm diffraction grating, a silver spherical mirror (R = 500 mm) and the DM in the focal plane of the mirror (see Fig. 1). The spherical mirror focuses the light also in the vertical direction avoiding beam clipping in the DM slit. The overall throughput of the shaper, including the grating losses, is ≈60%. The shaped pulses are fully characterized in amplitude and phase using Second Harmonic Generation – Frequency Resolved Optical Gating (SHG-FROG). Before introducing the pulse shaping, we used the DM to compress the near-IR NOPA pulse to its TL value. This is achieved by applying the phase-conjugation approach [16] which consists in retrieving the spectral phase of the uncompressed NOPA pulses by SHG-FROG and then applying to the mirror the deformation necessary to correct for it. With 4-5 iterations we can achieve 8.5fs pulsewidth [17], which closely approaches the 8.2 fs TL value.

4. Deformable mirror pulse shaping

To demonstrate the use of the push-pull DM for pulse shaping, we targeted the generation of pairs of short pulses with a controllable delay, in which the first pulse contains the blue components of the spectrum and the second the red ones (or vice versa). Such pulse pairs are useful for coherent control experiments, in particular for the pump-dump scheme [21] in which an excited state wavepacket created by the first pulse (pump pulse) is brought back down to the ground state by a second, suitably delayed and red-shifted pulse (dump pulse). In order to generate these pulses by simple spectral phase modulation, the easiest way is to create a triangular phase profile, in which the linear slopes give the time delay between the red and blue sub-pulses.

In order to take into account the real spectral shape of the pulse we used the Gerchberg-Saxton (GS) [22] algorithm to compute the required phase profile from the target time intensity profile. Figure 3(a) shows an example of GS result comparing the target (black line) and achievable (red line) pulse shape for a red-blue (RB) double pulse with 80fs separation. Small wings in the pulse are due to the irregular shape of the spectrum and to the use of phase-only modulation. Figure 3(b) shows the corresponding pulse spectrum and the spectral phase retrieved from the GS algorithm, which was then added to the one required for pulse

#132628 - $15.00 USD Received 30 Jul 2010; revised 17 Sep 2010; accepted 20 Sep 2010; published 19 Oct 2010

compression before applying it to the DM. It is interesting to note that it is easy to swap the red and blue components of the pulse, thereby generating a blue-red (BR) pulse, by simply changing the signs of the slopes of the triangular phase profile.

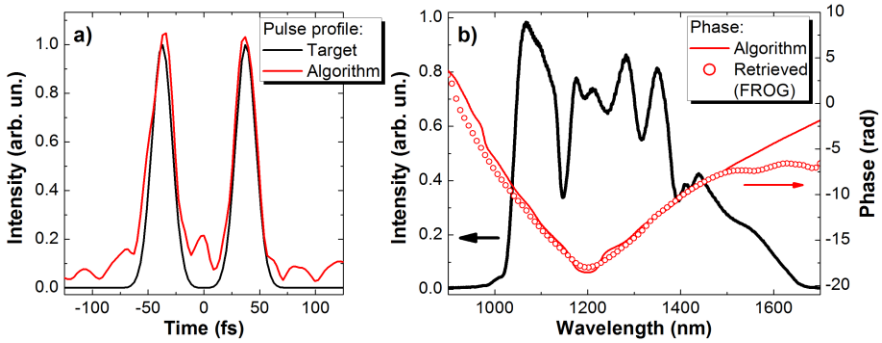

Fig. 3. (a) target (black line) profile of a double pulse and simulated profile after optimization with the GS algorithm (red line); (b) spectral intensity (solid black line) with spectral phases obtained by the algorithm (solid red line) and retrieved with the FROG measurement of the shaped pulse (circles) while the corresponding measured pulse intensity profile is plotted in Fig. 4(a) as the solid red line.

Figure 4(a) shows a sequence of BR double pulses with variable time delay created by the DM-based pulse shaper with just one iteration on the spectral phase. Measured pulse profiles are in good agreement with the ones simulated by the GS algorithm and display high contrast. By inverting the slopes of the two segments of the spectral phase profile, it is easy to swap the red and blue sub-pulses, as discussed above, thereby generating RB pulses (Fig. 4(b)). The time-frequency structure of such pulses is highlighted in Figs. 4(c)-4(d), which report the Husimi transforms [23] of two realizations, consisting of two relatively short (≈20 fs) sub-pulses spaced by 80 fs, with the blue sub-pulse preceding (Fig. 4(c)) or following (Fig. 4(d)) the red one.

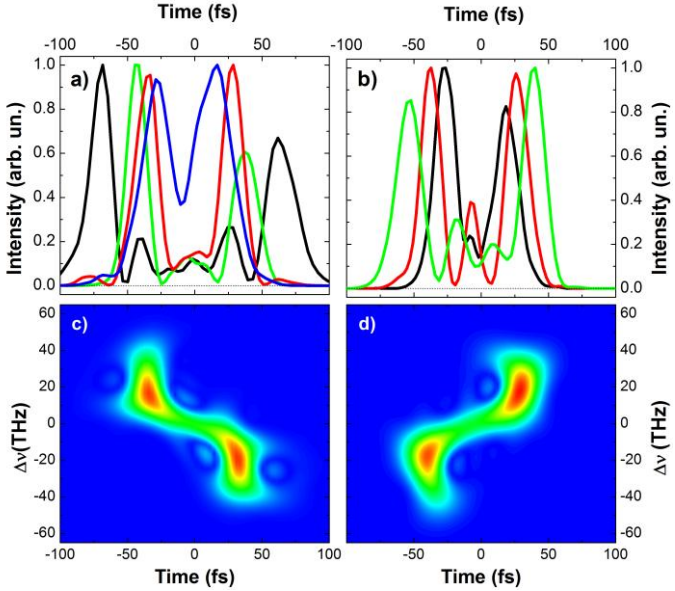

Fig. 4. (a) sequence of RB sub-pulses with variable temporal separation generated by the DM-based pulse shaper; (b) same as (a), with BR pulses. Husimi transforms of a BR (c) and RB (d) pulse sequence.

#132628 - $15.00 USD Received 30 Jul 2010; revised 17 Sep 2010; accepted 20 Sep 2010; published 19 Oct 2010

5. Application to coherent control

We have applied the DM to coherent control of ground to excited-state population transfer in the strong field limit, demonstrating that one can modify significantly the transmission spectrum and the population transferred to the excited state by simply acting on the spectral phase of the incident pulse. We used the laser dye LD690, which has been previously studied under high-intensity linearly chirped pulse excitation [24]. Figure 5(a) reports the absorption spectrum of LD690 in acetone (red line) together with the spectrum of the excitation pulses (blue line), generated by the visible NOPA. Before being shaped, the pulses are compressed to nearly TL duration by chirped mirrors [20]. The DM pulse shaper is based on the same setup used in the previous section for near-IR pulse shaping, thus demonstrating the frequency agility of our approach. The shaped pulses are focused on the LD690 solution in a 200-μm-thick cuvette. We measured, for different settings of the pulse shaper, the transmission spectrum of the solution as well as the time and frequency-integrated photoluminescence (PL), collected by a pair of off-axis parabolic mirrors.

We used the DM to create shaped BR and RB excitation pulses similar to those shown in Fig. 4. At low excitation intensity, the transmission spectrum and the PL intensity do not depend on the spectral phase of the excitation pulse. On the contrary, for high excitation intensities, both the transmission spectrum and the PL display a dramatic dependence on the spectral phase. Figure 5(b) shows the difference between the transmission spectra for BR and a RB shaped pulses (separated by 100 fs in both cases), normalized to the transmission of the RB pulse ($\Delta T/T = (T_{BR} - T_{RB})/T_{RB}$). One clearly sees for the BR pulse a large transmission increase (up to 40%) in the 620-670 nm spectral range, for which the dye absorption is negligible, and a corresponding absorption increase around 600 nm. This indicates that the red frequency components of the pulse experience gain at the expense of the blue components, in agreement with the intrapulse pump-dump mechanism proposed in [24,25]. Accordingly, the fluorescence intensity for the BR pulse drops by nearly 50% with respect to the RB one (see inset of Fig. 5(b)) because the red sub-pulse depletes the excited state population, created by the blue sub-pulse, through a stimulated emission process.

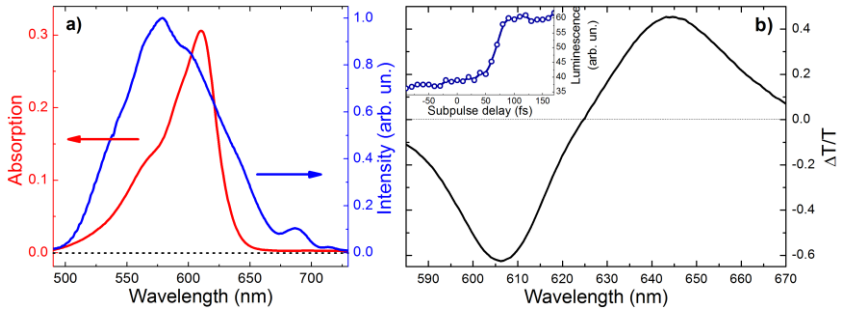

Fig. 5. (a) Absorption spectrum (red line) of LD690 in acetone and spectrum of the visible NOPA pulse (blue line); (b) difference between transmission spectra of BR and RB pulses. Inset shows fluorescence as a function of delay between red and blue sub-pulses.

6. Conclusion

In this paper we have introduced a novel device for programmable shaping of ultrabroadband pulses, based on a double-sided deformable mirror. While its shaping capabilities are limited in comparison with LC-SLMs and AOMs, it has important advantages such as the high throughput, the broad bandwidth acceptance supporting few-optical-cycle pulses and the capability of working over a very wide frequency range. We are convinced that this technique will find interesting application for a variety of coherent control experiments, especially in spectral ranges not easily accessible with other devices such as the mid-IR and the UV.

#132628 - $15.00 USD Received 30 Jul 2010; revised 17 Sep 2010; accepted 20 Sep 2010; published 19 Oct 2010